

Magneto thermoelastic stress in orthotropic hollow cylinders due to radially symmetric thermal and mechanical loads

H. L. Dai[†] and Y. M. Fu

Department of Engineering Mechanics, Hunan University, Changsha, 410082, Hunan Province, P. R. China

(Received October 17, 2005, Accepted July 3, 2006)

Abstract. In the paper, a direct method of solution of the Navier equation is presented. An orthotropic thick hollow cylinder under a one-dimensional steady-state temperature distribution and a uniform magnetic field with general types of thermal and mechanical boundary conditions is considered. The Navier equation in terms of displacement is derived and solved analytically by the direct method, and magneto thermoelastic responses and perturbation of the magnetic field vector in the orthotropic thick hollow cylinder is described. The present method is suitable for orthotropic thick hollow cylinders placed in an axial magnetic field with arbitrary thermal and mechanical boundary conditions. Finally, numerical examples are carried out and discussed.

Keywords: magneto thermoelastic; orthotropic hollow cylinder; perturbation of magnetic field vector.

1. Introduction

The increased use of orthotropic material in engineering applications has results in considerable research activity in this area in recent years. Nowinski (1957) generalized the Galerkin's problem to an orthotropic tube subjected to any axisymmetric temperature field. By means of employing the Frobenius series method, Mirsky (1964) was the first to study axisymmetric free vibrations of orthotropic cylindrical shells with infinite length based on three-dimensional elastic theory. Srinivas and Rao (1970) exactly investigated the bending, vibration and buckling of simply supported thick orthotropic rectangular plates and laminates based on a three-dimensional elasticity theory. Kalam and Tauchert (1978) investigated stresses in an orthotropic elastic cylinder due to a plane temperature distribution. The interaction between deformation and magnetic fields in a conducting orthotropic cylinder was considered by adding a Lorentz's electromagnetic force (Kraus 1984) into the equation of thermoelastic motion of an orthotropic cylinder in an axial magnetic field. Upadhyay and Mishra (1988) dealt with the non-axisymmetric dynamic behavior of buried orthotropic cylindrical shells excited by a combination of P-, SV- and Sh-waves. The elastodynamic solution for the thermal shock stress in an orthotropic thick cylindrical shell was presented by Cho *et al.* (1998). Abd-Alla *et al.* (1999) studied the transient thermal stresses in a rotating non-

[†] Corresponding author, E-mail: hldai520@sina.com

homogeneous cylindrically orthotropic composite tube and in a non-homogeneous spherically orthotropic elastic medium with spherical cavity, respectively. Dai and Wang (2004) presented an analytical solution for the interaction of electric potential, electric displacements, elastic deformations and mechanical loads, and described electromagnetoelastic responses and perturbation of magnetic field vector in a piezoelectric orthotropic hollow cylinder subjected to sudden mechanical load. The thermoelectroelastic responses were investigated by Dai *et al.* (2005) in orthotropic piezoelectric hollow cylinders subjected to thermal shock and electric excitation. To date, investigations on the magnetothermoelastic stress in orthotropic hollow cylinder due to radially symmetric loads have been few.

Finally, through numerical examples, it is concluded easily that stresses of an orthotropic thick hollow cylinder placed in an axial magnetic field, subjected to radially axisymmetric loads are not only dependent upon the thickness of the orthotropic hollow cylinder but also dependent on the magnetic field vector and the magnetic permeability in the orthotropic hollow cylinder.

2. Derivations

A long, orthotropic thick hollow cylinder placed initially in an axial magnetic field $\vec{H}(0, 0, H_z)$ is shown in Fig. 1. Consider a long, radial polarized thick hollow cylinder of inside radius a and outside radius b . We denote by r , the radial, θ , the circumferential, and z , the axial coordinate. Considering a generalized plane strain problem, the constitutive relations for the orthotropic thick hollow cylinder in cylindrical polar coordinate (r, θ, z) system are expressed as

$$\sigma_r = c_{11} \frac{\partial u}{\partial r} + c_{12} \frac{u}{r} - \lambda_1 T(r), \quad \sigma_\theta = c_{12} \frac{\partial u}{\partial r} + c_{22} \frac{u}{r} - \lambda_2 T(r) \quad (1a,b)$$

$$\lambda_1 = c_{11} \alpha_r + c_{12} \alpha_\theta, \quad \lambda_2 = c_{12} \alpha_r + c_{22} \alpha_\theta \quad (1c,d)$$

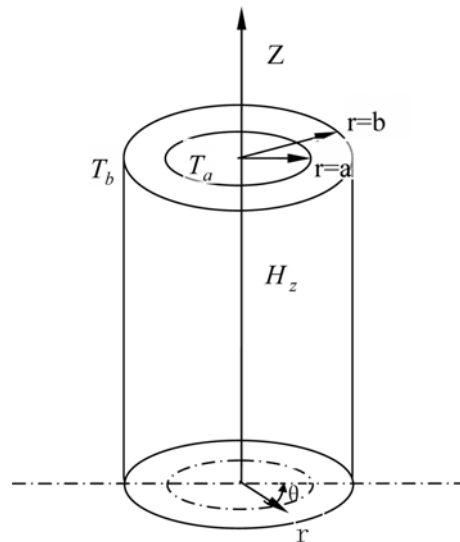


Fig. 1 A long orthotropic thick hollow cylinder

where c_{ij} ($i = 1, 2; j = 1, 2$) and α_i ($i = r, \theta$) are elastic constants and thermal expansion coefficients, respectively, u and σ_i ($i = r, \theta$) are the radial displacement and the component of stresses, respectively. $T(r)$ is temperature distribution determined from the heat conduction equation.

Assuming that the magnetic permeability, μ , (Ezzat 1997) of the orthotropic hollow cylinder equals the magnetic permeability of the medium around it, the governing electrodynamic Maxwell equations (Kraus 1984, Dai and Wang 2004) are given by

$$\vec{J} = \nabla \times \vec{h}, \quad \nabla \times \vec{e} = -\mu \frac{\partial \vec{h}}{\partial t}, \quad \text{div} \vec{h} = 0, \quad \vec{e} = -\mu \left(\frac{\partial \vec{U}}{\partial t} \times \vec{H} \right), \quad \vec{h} = \nabla \times (\vec{U} \times \vec{H}) \quad (2)$$

Applying an initial axial magnetic field vector $\vec{H}(0, 0, H_z)$ in cylindrical coordinate (r, θ, z) system to Eq. (3), yields

$$\vec{U} = (u, 0, 0), \quad \vec{e} = -\mu \left(0, H_z, \frac{\partial u}{\partial t} \right), \quad \vec{h} = (0, 0, h_z), \quad \vec{J} = \left(0, -\frac{\partial h_z}{\partial r}, 0 \right), \quad h_z = -H_z \left(\frac{\partial u}{\partial r} + \frac{u}{r} \right) \quad (3)$$

The magnetoelastostatic equilibrium equation of the orthotropic thick hollow cylinder is expressed as

$$\frac{\partial \sigma_r}{\partial r} + \frac{\sigma_r - \sigma_\theta}{r} + f_z = 0 \quad (4)$$

where f_z is defined as Lorentz's force (Kraus 1984, Dai and Wang 2004), which can be written as

$$f_z = \mu (\vec{J} \times \vec{H}) = \mu H_z^2 \frac{\partial}{\partial r} \left(\frac{\partial u}{\partial r} + \frac{u}{r} \right) \quad (5)$$

Substituting Eqs. (1) into Eq. (4) and utilizing Eq. (5), the Navier equation in term of the displacement is

$$\frac{\partial^2 u}{\partial r^2} + \frac{1}{r} \frac{\partial u}{\partial r} - M \frac{1}{r^2} u = N \left[\lambda_1 \frac{\partial T}{\partial r} + (\lambda_1 - \lambda_2) \frac{T}{r} \right] \quad (6)$$

where $M = \frac{c_{22} + \mu H_z^2}{c_{11} + \mu H_z^2}$ and $N = \frac{1}{c_{11} + \mu H_z^2}$.

3. Heat conduction problem

Consider the orthotropic thick hollow cylinder with temperature T_a at the inside at the inside surface, T_b at the outside at the outside surface. The heat conduction equation in the steady-state condition for the one-dimensional problem in polar coordinates and the thermal boundary conditions for the orthotropic thick hollow cylinder are given, respectively, as (Obata 1994, Jabbari 2002)

$$\frac{1}{r} \frac{\partial}{\partial r} \left(r \frac{\partial T(r)}{\partial r} \right) = 0, \quad (a \leq r \leq b) \quad (7)$$

$$T = T_a \quad \text{at} \quad r = a; \quad T = T_b \quad \text{at} \quad r = b \quad (8)$$

Then the general solution of the Eq. (7) is given by

$$T(r) = A_1 \ln r + A_2 \quad (9)$$

Using the boundary conditions (8) to determine the constants A_1 and A_2 , yields

$$A_1 = \frac{T_b - T_a}{\ln b - \ln a}, \quad A_2 = \frac{T_a \ln b - T_b \ln a}{\ln b - \ln a} \quad (10)$$

4. Solution of the Navier equation

Substituting Eq. (9) into Eq. (6), yields

$$\frac{\partial^2 u}{\partial r^2} + \frac{1}{r} \frac{\partial u}{\partial r} - M \frac{1}{r^2} u = A_3 \frac{1}{r} + A_4 \frac{\ln r}{r} \quad (11)$$

where

$$A_3 = N[\lambda_1 A_1 + (\lambda_1 - \lambda_2) A_2], \quad A_4 = N(\lambda_1 - \lambda_2) A_1 \quad (12)$$

Eq. (11) is the Euler differential equation with homogeneous and inhomogeneous solutions. It is obvious that the homogeneous solution to Eq. (11) can be obtained by assuming

$$u = Cr^\beta \quad (13)$$

where C is an arbitrary constant. Substituting Eq. (13) into Eq. (11) and omitting the right-hand side, one obtains

$$\beta^2 - M = 0 \quad (14)$$

Eq. (14) has two real roots β_1, β_2 :

$$\beta_{1,2} = \pm \sqrt{M} \quad (15)$$

Thus the homogeneous solution is

$$u^h(r) = B_1 r^{\beta_1} + B_2 r^{\beta_2} \quad (16)$$

The nonhomogeneous solution $u^n(r)$ is assumed to be of the form

$$u^n(r) = D_1 r + D_2 r \ln r \quad (17)$$

Substituting Eq. (17) into Eq. (11), yields

$$D_1 = \frac{A_3(1-M) - 2A_4}{(1-M)^2}, \quad D_2 = \frac{A_4}{1-M} \quad (18)$$

The complete solution for $u(r)$ is the sum of the homogeneous and nonhomogeneous solution as

$$u(r) = u^h(r) + u^n(r) = B_1 r^{\beta_1} + B_2 r^{\beta_2} + D_1 r + D_2 r \ln r \quad (19)$$

Substituting Eq. (19) into Eqs. (1a,b) and the last term of Eq. (3), the stresses and perturbation of magnetic field vector of the orthotropic thick hollow cylinder are obtained as

$$\begin{aligned} \sigma_r = & (c_{11}\beta_1 + c_{12})B_1 r^{\beta_1-1} + (c_{11}\beta_2 + c_{12})B_2 r^{\beta_2-1} + (c_{11} + c_{12})D_1 + c_{11}D_2 \\ & + (c_{11} + c_{12})D_2 \ln r - \lambda_1(A_1 \ln r + A_2) \end{aligned} \quad (20a)$$

$$\begin{aligned} \sigma_\theta = & (c_{12}\beta_1 + c_{22})B_1 r^{\beta_1-1} + (c_{12}\beta_2 + c_{22})B_2 r^{\beta_2-1} + (c_{12} + c_{22})D_1 + c_{12}D_2 \\ & + (c_{12} + c_{22})D_2 \ln r - \lambda_2(A_1 \ln r + A_2) \end{aligned} \quad (20b)$$

$$h_z = -H_z[(\beta_1 + 1)B_1 r^{\beta_1-1} + (\beta_2 + 1)B_2 r^{\beta_2-1} + 2D_1 + D_2 + 2D_2 \ln r] \quad (20c)$$

To determine the constants B_1 and B_2 , consider the boundary conditions for stresses given by

$$\sigma_r(a) = -p_a, \quad \sigma_r(b) = -p_b \quad (21)$$

Substituting the boundary conditions (21) into Eq. (20), the constants of integration become

$$B_1 = \frac{d_5 b^{\beta_2-1} - d_6 a^{\beta_2-1}}{d_1(a^{\beta_1-1} b^{\beta_2-1} - a^{\beta_2-1} b^{\beta_1-1})} \quad (22a)$$

$$B_2 = \frac{d_5 b^{\beta_1-1} - d_6 a^{\beta_1-1}}{d_2(a^{\beta_2-1} b^{\beta_1-1} - a^{\beta_1-1} b^{\beta_2-1})} \quad (22b)$$

where

$$\begin{aligned} d_1 = & c_{11}\beta_1 + c_{12}, \quad d_2 = c_{11}\beta_2 + c_{12}, \quad d_3 = (c_{11} + c_{12})D_1 + c_{11}D_2 - \lambda_1 A_2 \\ d_4 = & (c_{11} + c_{12})D_2 - \lambda_1 A_1, \quad d_5 = -p_a - d_3 - d_4 \ln a, \quad d_6 = -p_b - d_3 - d_4 \ln b \end{aligned} \quad (23)$$

5. Numerical examples and discussions

In the numerical calculations, the material constants for orthotropic thick hollow cylinders are taken as (Dai and Wang 2004):

$$\begin{aligned} c_{11} = c_{33} = & 110.0 \text{ GPa}, \quad c_{12} = 77.8 \text{ GPa}, \quad c_{13} = c_{23} = 115.0 \text{ GPa} \\ c_{22} = & 220.0 \text{ GPa}, \quad \alpha_r = 1.0 \times 10^{-6} (1/^\circ\text{C}), \quad \alpha_\theta = 1.2 \times 10^{-5} (1/^\circ\text{C}) \\ \mu = & 4\pi \times 10^{-7} (\text{H/m}) \quad \text{and} \quad H_z = 1.796 \times 10^{-9} (\text{A/m}) \end{aligned}$$

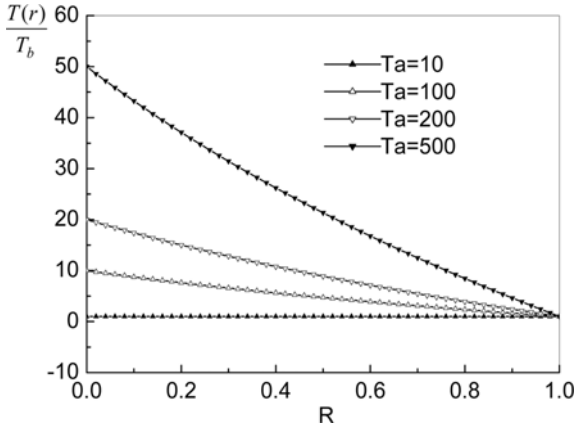


Fig. 2 Radial distribution of temperature at $T_a = 10^\circ\text{C}$, $T_a = 100^\circ\text{C}$, $T_a = 200^\circ\text{C}$ and $T_a = 500^\circ\text{C}$, where $R = (r - a)/(b - a)$ and $b/a = 2$

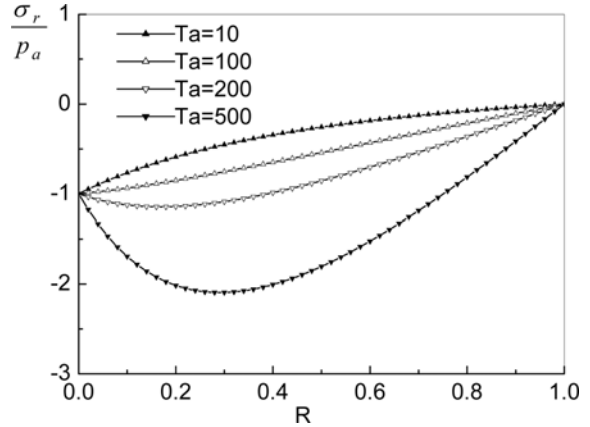


Fig. 3 Radial distribution of radial stress at $T_a = 10^\circ\text{C}$, $T_a = 100^\circ\text{C}$, $T_a = 200^\circ\text{C}$ and $T_a = 500^\circ\text{C}$, where $R = (r - a)/(b - a)$ and $b/a = 2$

The internal boundary condition for temperature is assumed as $T_a = 10^\circ\text{C}$, 100°C , 200°C , and 500°C , respectively, and the external boundary condition for temperature is taken as $T_b = 10^\circ\text{C}$. The orthotropic thick hollow cylinder has pressure on its inner surface so the boundary conditions for stresses are taken as $\sigma_a = -50 \text{ MPa}$ and $\sigma_b = 0 \text{ MPa}$. The internal radius of orthotropic cylinders is taken as $a = 0.01 \text{ m}$.

Example 1: The ratio of internal radius to external radius is taken as $b/a = 2$, and the dimensionless radial coordinate is taken as $R = (r - a)/(b - a)$. Fig. 2 shows temperature distribution at $T_a = 10^\circ\text{C}$, 100°C , 200°C and 500°C along the radial direction of the orthotropic thick hollow cylinder. From the curve of the figure, it is seen easily that temperature show weakly non-linear distribution with the increasing of temperature along the radial direction of the orthotropic hollow cylinder. Figs. 3-5 show stresses and perturbation of magnetic field vector distribution at

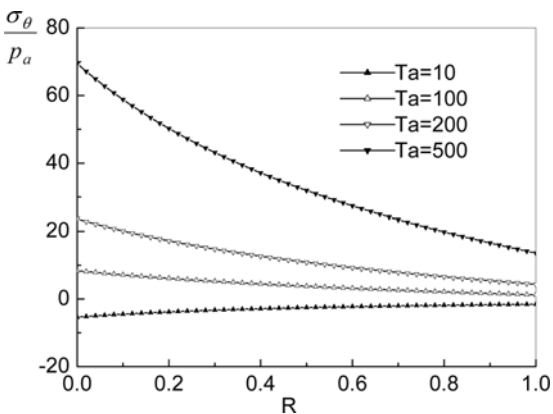


Fig. 4 Radial distribution of hoop stress at $T_a = 10^\circ\text{C}$, $T_a = 100^\circ\text{C}$, $T_a = 200^\circ\text{C}$ and $T_a = 500^\circ\text{C}$, where $R = (r - a)/(b - a)$ and $b/a = 2$

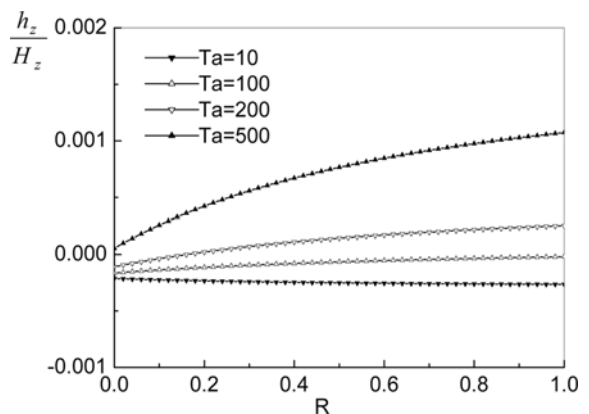


Fig. 5 Radial distribution of perturbation of magnetic field vector at $T_a = 10^\circ\text{C}$, $T_a = 100^\circ\text{C}$, $T_a = 200^\circ\text{C}$ and $T_a = 500^\circ\text{C}$, where $R = (r - a)/(b - a)$ and $b/a = 2$

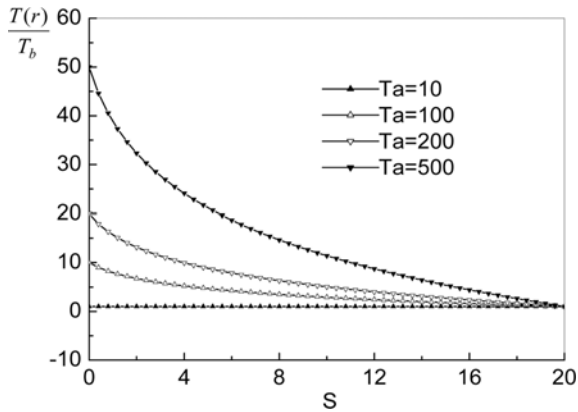


Fig. 6 Radial distribution of temperature at $T_a = 10^\circ\text{C}$, $T_a = 100^\circ\text{C}$, $T_a = 200^\circ\text{C}$ and $T_a = 500^\circ\text{C}$, where $S = (r - a)/a$ and $b/a = 21$

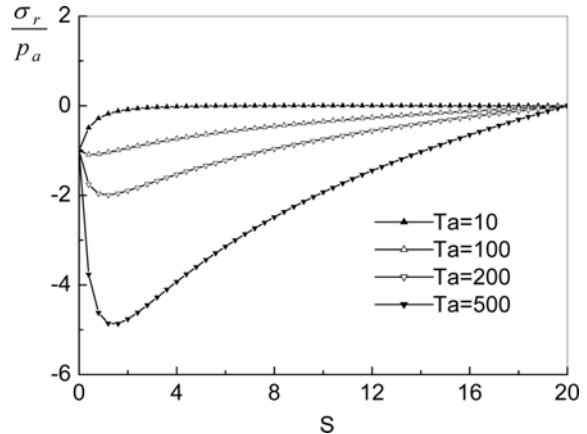


Fig. 7 Radial distribution of radial stress at $T_a = 10^\circ\text{C}$, $T_a = 100^\circ\text{C}$, $T_a = 200^\circ\text{C}$ and $T_a = 500^\circ\text{C}$, where $S = (r - a)/a$ and $b/a = 21$

$T_a = 10^\circ\text{C}$, 100°C , 200°C and 500°C along the radial direction of the orthotropic thick hollow cylinder, respectively. From Fig. 3, it is seen that the radial stresses at the boundaries $R = 0, 1$ satisfy the given boundary conditions with different temperatures, and the magnitude of value becomes large with the increasing of temperature. When $T_a = 500^\circ\text{C}$, the maximum radial stress -2.09 occurs at the neighborhood of $R = 0.3$. It is seen easily from Fig. 4 that the hoop compression stress become tensile stress with the increasing of temperature in the orthotropic hollow cylinder, and the amplitude of the hoop stress is larger than the amplitude of the radial stress in the orthotropic hollow cylinder. From the curve, it is also seen that hoop stresses show weakly non-linear distribution with the increasing of temperature along the radial direction of the orthotropic hollow cylinder, and the peak value of hoop stress occur at the internal wall of orthotropic hollow cylinder. From Fig. 5, it is shown that the values of perturbation of magnetic field vector increase gradually from the inner-wall to the outer-wall, and the values become larger at the same point with the increase of temperature.

Example 2: The ratio of internal radius to external radius is taken as $b/a = 21$, and the dimensionless radial coordinate is taken as $S = (r - a)/a$. Figs. 6-9 show temperature, stresses and perturbation of magnetic field vector distribution at $T_a = 10^\circ\text{C}$, 100°C , 200°C and 500°C along the radial direction of the orthotropic thick hollow cylinder, respectively. From Fig. 6, it is seen easily that the temperature distribution are the similar as example 1. From Fig. 7, it is seen that the radial stresses at the boundaries $R = 0, 1$ satisfy the given boundary conditions with different temperatures. It is also seen from the curve that the radial tensile stress become compression stress with the increasing of temperature in the orthotropic hollow cylinder, and the peak value of radial stresses occur at the neighborhood of $S = 1.4$ with different temperatures. When $T_a = 500^\circ\text{C}$, the peak value of radial stress is -4.86 , it is about two times larger than that of example 1. From Fig. 8, it is seen easily that the hoop stresses are the similar as example 1. It is also seen from the curve that the hoop value is smaller than that of example 1. From Fig. 9, it is shown that the values of perturbation of magnetic field vector decrease gradually from the inner-wall to the outer-wall, and the hoop values occur the internal wall of the orthotropic hollow cylinder with different temperatures.

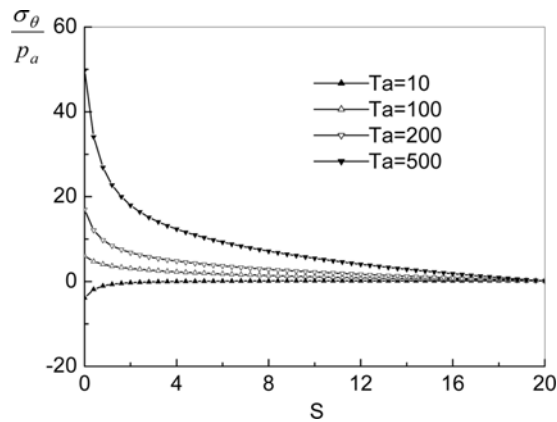


Fig. 8 Radial distribution of hoop stress at $T_a = 10^\circ\text{C}$, $T_a = 100^\circ\text{C}$, $T_a = 200^\circ\text{C}$ and $T_a = 500^\circ\text{C}$, where $S = (r - a)/a$ and $b/a = 21$

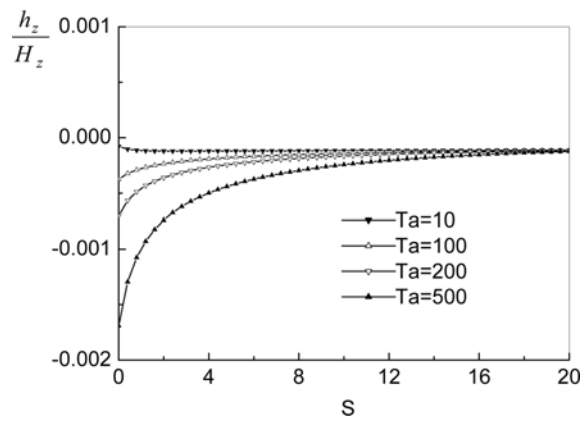


Fig. 9 Radial distribution of perturbation of magnetic field vector at $T_a = 10^\circ\text{C}$, $T_a = 100^\circ\text{C}$, $T_a = 200^\circ\text{C}$ and $T_a = 500^\circ\text{C}$, where $S = (r - a)/a$ and $b/a = 21$

6. Conclusions

- (1) The article presents an analytical solution for the calculation of the axisymmetric magnetoelastostatic stresses in orthotropic thick hollow cylinders. In contrast to the tradition potential function method, which exhibits some limitations in choosing the boundary conditions for stresses and displacements, the direct method presented in the paper does not have any limitation to handle the general types of mechanical and thermal boundary conditions.
- (2) Comparing two numerical examples, it can be concluded that different thickness of wall have great effect on the stresses distribution in the orthotropic thick hollow cylinder due to radially symmetric load, so it can tailor the design of engineering.

References

- Abd-Alla, A.M., Abd-Alla, A.N. and Zeidan, N.A. (1999), "Transient thermal stress in a rotation non-homogeneous cylindrically orthotropic composite tube", *Appl. Mathematic and Computation*, **105**, 253-269.
- Cho, H., Kardomates, G.A. and Valle, C.S. (1998), "Elastodynamic solution for the thermal shock stresses in an orthotropic thick cylindrical shell", *J. Appl. Mech.*, **65**, 184-193.
- Dai, H.L. and Wang, X. (2004), "Dynamic responses of piezoelectric hollow cylinders in an axial magnetic field", *Int. J. Solids Struct.*, **41**, 5231-5246.
- Dai, H.L., Wang, X. and Dai, Q.H. (2005), "Thermoelectroelastic responses in orthotropic piezoelectric hollow cylinders subjected to thermal shock and electric excitation", *J. of Reinforced Plastics and Composites*, **24**(10), 1085-1102.
- Ezzat, M.A. (1997), "Generation of generalized magnetoelastostatic waves by thermal shock in a perfectly conducting half-space", *J. Thermal Stresses*, **20**(6), 917-933.
- Jabbari, M., Sohrabpour, S. and Eslami, M.R. (2002), "Mechanical and thermal stresses in a functionally graded hollow cylinder due to radially symmetric loads", *Int. J. Pressure Vessels and Piping*, **79**, 493-497.
- Kalam, M.A. and Tauchert, T.R. (1978), "Stresses in an orthotropic elastic cylinder due to a plane temperature distribution", *J. Thermal Stresses*, **1**, 13-24.

- Kraus, J.D. (1984), *Electromagnetics*, McGrawHill, Inc. U.S.A.
- Mirsky, I. (1964), "Axisymmetric vibrations of orthotropic cylinders", *J. Acoust. Soc. Am.*, **36**, 2106-2112.
- Nowinski, J. (1957), "Thermoelastic states in a thick-walled orthotropic cylinder surrounded by an elastic medium", *Bull 1' Academic Polonaise Sciences*, **5**, 19-22.
- Obata, Y. and Noda, N. (1994), "Steady thermal stresses in a hollow circular cylinder and a hollow sphere of a functionally gradient material", *J. Thermal Stresses*, **17**, 471-487.
- Srinivas, S. and Rao, A.K. (1970), "Bending, vibration and buckling of simply supported thick orthotropic rectangular plates and laminates", *Int. J. Solids Struct.*, **6**(11), 1463-1481.
- Upadhyay, P.C. and Mishra, B.K. (1988), "Non-axisymmetric dynamic response of buried orthotropic cylindrical shells", *J. Sound Vib.*, **121**, 149-160.

Notation

- \vec{U}, u : displacement vector and radial displacement [m]
 c_{ij} : elastic constants [N/m²]
 σ_i : the component of stresses [N/m²]
 f_z : Lorentz's force [kg/m²s²]
 r : radius [m]
 a, b : inner and outer radii of the orthotropic hollow cylinder [m]
 μ : magnetic permeability [H/m]
 \vec{H} : magnetic intensity vector (0, 0, H_z)
 \vec{h} : perturbation of magnetic field vector (0, 0, h_z)
 \vec{J} : electric current density vector
 \vec{e} : perturbation of electric field vector